Proceedings of the Combustion Institute, Volume 28, 2000/pp. 245–252

REACTION ZONE STRUCTURE OF NON-PREMIXED TURBULENT FLAMES IN THE "INTENSELY WRINKLED" REGIME

A. RATNER,[1] J. F. DRISCOLL,[1] J. M. DONBAR,[2] C. D. CARTER[3] AND J. A. MULLIN[1]
[1]*Department of Aerospace Engineering*
University of Michigan
Ann Arbor, MI 48109, USA
[2]*AFRL/PRSS*
Wright-Patterson Air Force Base
Dayton, OH 45433, USA
[3]*Innovative Scientific Solutions, Inc.*
Dayton, OH 45440, USA

Simultaneous images of the CH and OH reaction zones are reported for "Intensely Wrinkled" non-premixed flames, to determine whether reaction zones retain their thin "laminar flamelet" structure or become "distributed reaction zones." Intensely Wrinkled Flames (IWFs) were achieved by using a special burner with large coflow air velocities to obtain a normalized turbulence intensity ($u'/\bar{U}$) of 3.6, which is 10 times greater than the turbulence intensity within jet flames. The images were used to measure profiles of the flame surface density (Σ) and the average CH layer thickness ($\bar{\delta}_{CH}$); it is argued that these parameters are the ones that should be used to assess new large eddy simulations (LESs), rather than insensitive parameters such as mean concentrations.

In the regime of IWFs, the CH reaction zones remained as thin as those measured in laminar jet flames (i.e., less than 1 mm thick) and had the appearance of flamelets. These thin reaction zones were extinguished before they became thickened by intense turbulence, which provides experimental evidence to support laminar flamelet modeling concepts. "Shredded flames" occurred, within which the reaction zones were short, discontinuous segments, and the degree of flame wrinkling was significantly larger than in jet flames. Shredded flames have not been observed previously. There is no evidence of small-scale wrinkling of the reaction zones at scales less than half the integral scale. The images showed where the instantaneous stoichiometric contour is located, since it exists at the boundary between the CH and OH layers. Flame surface densities were typically 0.3 mm^{-1}.

Introduction

The goal of the present work was to study flames in the intensely wrinkled flame (IWF) regime, which differ from turbulent jet flames in that the value of the turbulence intensity ($u'/\bar{U}$) is typically 3.6, which is 10 times that of any turbulent jet flame. Images of the CH and OH reaction zones have not been available for flames in this IWF regime, so simultaneous images of the CH and OH layers were recorded and used to measure the profiles of the flame surface density (Σ) and the average thickness of the CH layers ($\bar{\delta}_{CH}$). An IWF was produced by using high-velocity coflow air (with swirl) to produce a central recirculation zone and conditions similar to those within a gas-turbine combustor. Some locations have low mean velocities, and the turbulent eddies have large residence times in the reaction layers, so the layers can "roll up" in the eddies and become intensely wrinkled and locally extinguished. The structure of such IWFs is shown to be different from jet flames.

The reported measurements of surface density (Σ) and the CH layer thickness ($\bar{\delta}_{CH}$) provide a useful way to assess new large eddy simulations (LESs) of IWFs, since surface density provides a sensitive measure of whether or not the structure is simulated correctly, whereas other parameters such as mean temperature do not. Several recent LESs consider conditions with some similarities to the present experiment. Kim et al. [1] used an LES model and flamelet assumptions to simulate a generic gas-turbine combustor having coaxial air, swirl, and internal recirculation. Menon and Jou [2] used the same LES model to simulate a ramjet combustor. Dahm et al. [3] reported images of the instantaneous reaction zones that were computed using a local integral moment simulation of the same combustor that was used in the present study. They used an unsteady discrete vortex method to simulate the velocity field and solved the unsteady integral form of the flamelet equations [4] along the wrinkled stoichiometric contour. Although their flow conditions were not

Report Documentation Page

Form Approved
OMB No. 0704-0188

Public reporting burden for the collection of information is estimated to average 1 hour per response, including the time for reviewing instructions, searching existing data sources, gathering and maintaining the data needed, and completing and reviewing the collection of information. Send comments regarding this burden estimate or any other aspect of this collection of information, including suggestions for reducing this burden, to Washington Headquarters Services, Directorate for Information Operations and Reports, 1215 Jefferson Davis Highway, Suite 1204, Arlington VA 22202-4302. Respondents should be aware that notwithstanding any other provision of law, no person shall be subject to a penalty for failing to comply with a collection of information if it does not display a currently valid OMB control number.

1. REPORT DATE	2. REPORT TYPE	3. DATES COVERED
04 AUG 2000	**N/A**	**-**

4. TITLE AND SUBTITLE	5a. CONTRACT NUMBER
Reaction Zone Structure of Non-Premixed Turbulent Flames in the Intensely Wrinkled Regime	5b. GRANT NUMBER
	5c. PROGRAM ELEMENT NUMBER
6. AUTHOR(S)	5d. PROJECT NUMBER
	5e. TASK NUMBER
	5f. WORK UNIT NUMBER
7. PERFORMING ORGANIZATION NAME(S) AND ADDRESS(ES) **Department of Aerospace Engineering University of Michigan Ann Arbor, MI 48109, USA; AFRL/PRSS Wright-Patterson Air Force Base Dayton, OH 45433, USA**	8. PERFORMING ORGANIZATION REPORT NUMBER
9. SPONSORING/MONITORING AGENCY NAME(S) AND ADDRESS(ES)	10. SPONSOR/MONITOR'S ACRONYM(S)
	11. SPONSOR/MONITOR'S REPORT NUMBER(S)

12. DISTRIBUTION/AVAILABILITY STATEMENT
Approved for public release, distribution unlimited

13. SUPPLEMENTARY NOTES
See also ADM001790, Proceedings of the Combustion Institute, Volume 28. Held in Edinburgh, Scotland on 30 July-4 August 2000. , The original document contains color images.

14. ABSTRACT

15. SUBJECT TERMS

16. SECURITY CLASSIFICATION OF:			17. LIMITATION OF ABSTRACT	18. NUMBER OF PAGES	19a. NAME OF RESPONSIBLE PERSON
a. REPORT	b. ABSTRACT	c. THIS PAGE			
unclassified	**unclassified**	**unclassified**	**UU**	**8**	

Standard Form 298 (Rev. 8-98)
Prescribed by ANSI Std Z39-18

matched with this experiment, their computed reaction zones have an appearance that is remarkably similar to the present images. No quantitative comparisons of the present measurements to LESs can be made at present because LES studies have yet to report computed values of flame surface density and reaction layer thickness.

Another motivation for imaging the reaction zones was to determine the range of operating conditions that certain reactions are confined to thin flamelets, and conditions for which they are not. Bilger [5] predicted that for certain high-turbulence intensity conditions, reaction zones will no longer be flamelet-like but become quasi-equilibrium distributed reaction zones. Peters [6] predicted that for certain conditions, intense turbulence can create strain rates and scalar dissipation rates which may force the flamelets to become thinner. Previously, several of the authors of this paper studied a turbulent jet flame (Carter et al. [7], Donbar et al. [8]) which used a different apparatus than was used in the present work (the jet flame used in Refs. [7] and [8] did not have coflowing air, swirl, or internal recirculation). Within the jet flame of Refs. [7] and [8], numerous images of CH and OH radicals were obtained at a high Reynolds number of 18,600; the CH layers in the jet flame were found to be less than 1 mm thick and were thinner than CH layers in a laminar jet flame. Thus, turbulence did not broaden the CH layers in the jet flames of Refs. [7] and [8]. The OH concentration field was spread out over broad regions in Refs. [7] and [8], but this does not imply that the flame is distributed in space. OH occurs wherever hot water vapor exists; for example, downstream of a flat premixed flame, OH will occur in the product gases for several centimeters, but this OH region is not considered part of the flame itself.

Previous studies of CH layers near the base of a jet flame were conducted by Starner et al. [9] and Schefer et al. [10]. Seitzmann et al. [11] reported images of the structure of OH zones, while Barlow and Frank [12] drew conclusions about turbulent transport based on single-point measurements. However, all these findings are limited to jet flames, which have turbulence intensities ($u'/\bar{U}$) that do not exceed 0.3. In jet flames, the relatively large mean velocity $\bar{U}$ convects eddies through the reaction zone before they can severely wrinkle and broaden the reaction layers. Information about flamelet structure from experiments is needed to assess the validity of numerical simulations that employ flamelet concepts, such as the models of Mahalingham et al. [13], Pitsch et al. [14], Pope and Anand [15], and Van Kalmthout et al. [16].

Experimental Apparatus

Figure 1a shows the IWF burner. The geometry is simple and axisymmetric, and the profiles of inlet-plane properties were carefully quantified during the University of Michigan/GRI/IFRF Scaling 400 studies [17]. Fuel is injected along the centerline from a central circular fuel tube of 10 mm inner diameter; coaxial air with a high-speed axial velocity of 18 m/s issues from a 27 mm diameter circular air tube. Swirl is added to the airstream with a movable block swirler [17]; the swirl number, as defined in Ref. [17], is 1.0. An internal recirculation zone causes the flame to be intense and short, with a length of 65 mm. The global Reynolds number (U^*d^*/ν^*) of the flame is 26,200, which is based on the Thring-Newby [18] effective jet diameter d^*. U^* is $(4\ m_o)/(\pi\rho d^{*2})$ and has a value of 17 m/s, where m_o is the total mass flow rate issuing from the coaxial fuel and air tubes. The effective jet diameter, d^*, is $2m_o/(\pi\rho J_o)^{1/2}$ and has a value of 23 mm, where J_o is the momentum per second issuing from the coaxial fuel and air tubes. The fuel is 16% methane and 84% nitrogen, by mass, and the oxidizer is 41% O_2 and 59% N_2, to eliminate the formation of soot precursors, which could interfere with CH fluorescence [19]. Integral scales (ℓ) in the flame were measured using particle imaging velocimetry (PIV) diagnostics; they varied from 7.6 mm to 19.3 mm. The local Reynolds number ($u'\ \ell/\nu$) was typically 350.

Figure 2 shows the simultaneous CH/OH planar laser-induced fluorescence (PLIF) system used. The 390 nm output of a Nd:YAG-pumped dye laser was tuned to the $Q_1(7.5)$ transition of the $B^2\Sigma^-$-$X^2\Pi$ ($v' = 0$, $v'' = 0$) band of CH. CH fluorescence was recorded from 420 to 440 nm from the A-X (1,1), (0,0) and B-X (0,1) bands. A 30 mm × 20 mm region on the 230 μm thick light sheet was focused onto a Princeton Instruments intensified charge-coupled device array camera having 576 × 384 pixels using a 58 mm/f1.2 lens. Each 3-by-3 pixel region was averaged; the distance imaged on three pixels is 156 μm. The 281.34 nm output of a second Nd:YAG-pumped dye laser was tuned to the R_1 (8.5) transition of the $A^2\Sigma^+$-$X^2\Pi$ ($v' = 1$, $v'' = 0$) band of OH, and OH fluorescence was collected from the A-X (1,1) and (0,0) bands at 306–320 nm. The spatial resolution of the PLIF system was the laser sheet thickness of 0.23 mm, and this resolution was sufficiently small such that it did not have any effect on the conclusions of the study.

Results

The Visible Structure of the CH and OH Reaction Zones

Figure 3b shows that the measured turbulence intensity ($u'/\bar{U}$) varies from 2.5 to 17.7 within the boxed region shown in the upper left in Fig. 3a; u' is defined as the root-mean-squared velocity fluctuation. Turbulence intensity has an average value of 3.6 in this region in the IWF, whereas numerous

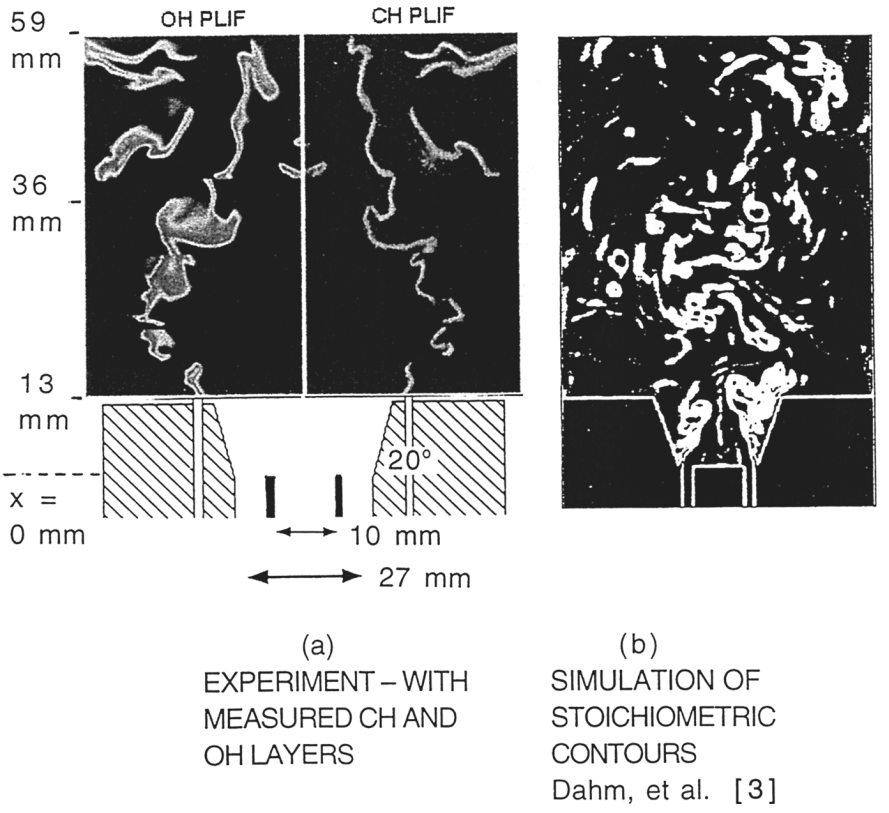

FIG. 1. Geometry of the intensely wrinkled flame (a) showing some OH and CH reaction layers, compared with (b) large eddy (LIM) Simulation of stoichiometric contours of Dahm et al. [3,4]. Note: Quantitative comparisons are not possible since simulation flow conditions are not matched to experiment. Reynolds number $U^*d^*/\nu^* = 26{,}200$; coflow air velocity = 18 m/s.

studies have shown that the corresponding value in jet flames rarely exceeds 0.3 [8]. Also shown are some mean velocity profiles. The PIV system that was used is described in Refs. [7] and [8].

Figure 4 shows simultaneous images of the CH and OH reaction zones that occur at three random times. By comparing the top two images in Fig. 4, it is seen that each CH layer is adjacent to an OH layer. Therefore the instantaneous stoichiometric contour can be determined from the CH/OH images in Fig. 4. The stoichiometric contour occurs at the boundary between the CH and OH regions; it is the edge of the CH layer which is in contact with an OH layer. To assess the validity of this concept, counterflow flame calculations with full CH chemistry were performed [8], and they showed that the peak value of CH concentration always exists on the fuel-rich side of the stoichiometric contour. The peak values of OH always exist on the fuel-lean side, and the stoichiometric contour always lies between the peak values of CH and OH, for any strain rate. Some other observations that can be deduced from Fig. 4 are the following.

1. The CH reaction layers remain thin and have a thickness of less than 1 mm. As shown below, the CH layers in the IWF are no thicker than CH layers in a laminar jet flame.
2. Frequent "shredding" of the CH reaction layers into short, discontinuous segments occurs, which has not been seen in jet flames. In the present experiment the CH and OH layers nearly always disappear together, so it is argued that the flame chemistry has been locally extinguished between the observed flame segments. If only the CH (or only the OH) layer was to disappear, it could not be argued that the flame was extinguished; however, both layers tend to extinguish together. In jet flames, some "holes" are seen, but jet flames have not displayed the large number of local extinction regions to create the many short layers that are seen in Fig. 4.

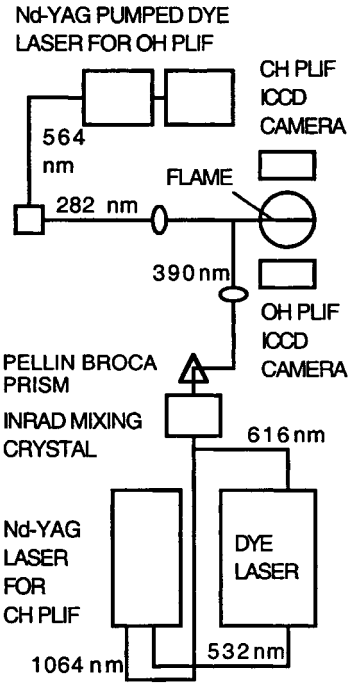

FIG. 2. Schematic of the simultaneous CH/OH planar laser-induced fluorescence (PLIF) diagnostics used.

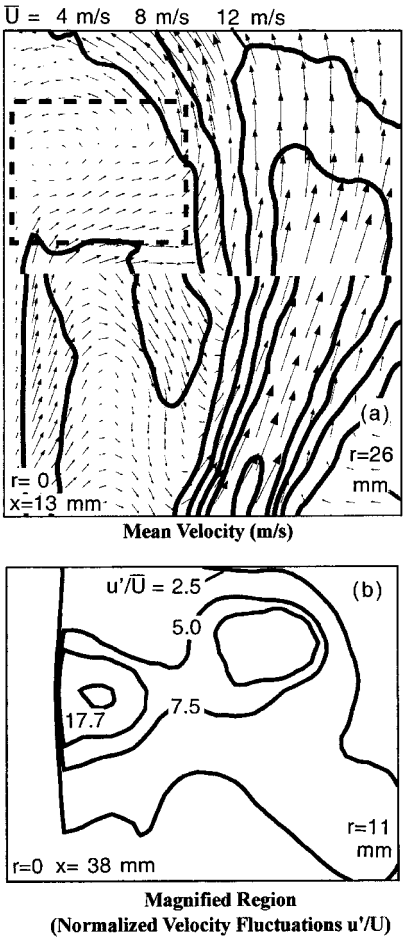

FIG. 3. Measured mean velocity (a) in the region r = 0–26 mm and x = 13–44 mm; (b) turbulence intensity ($u'/\bar{U}$) within the boxed region shown in the upper left. Average value $u'/\bar{U}$ in the boxed region is 3.6, which is 10 times that of a jet flame. Average value of $\bar{U}$ in box is 1.5 m/s.

3. "Distributed reaction zones" are not observed for the CH reactions that occur in the present high-turbulence intensity conditions. The CH layer is doubled in thickness where layers are merging or are curved but remains relatively thin. The present results do not imply that distributed CH reactions cannot occur for other conditions.
4. The OH reaction zones appear to be layerlike but are not as thin as the CH layers. OH layers are typically 1 mm thick where they are not merged and are up to 4 mm thick where they merge together. The OH layers are often shredded into short, discontinuous segments, as are the CH layers.
5. The wrinkling of the reaction layers is more intense than seen in jet flames [8], and the qualitative wrinkled structure is similar to the unsteady LIM model simulation of Dahm et al. [3,4] which is shown in Fig. 1b for this geometry. Quantitative comparison to the simulation of Ref. [3] is not possible since velocities and fuel types were not matched.
6. Numerous pockets are seen, which appear as islands of fluid surrounded by CH layers in the three CH images on the left side of Fig. 4. Five pockets can be identified in the three CH images; inspection of the OH images on the right side of Fig. 4 shows that some of the pockets contain OH (implying that they contain oxidizer), while other pockets contain no OH, which implies they contain fuel-rich gases.
7. Large flame curvature and cusp regions are more frequently observed in Fig. 4 than in jet flames [8].

The reaction zones in Fig. 4 are intensely wrinkled and shredded because the *residence time* of the reaction layers within each large-scale vortex is large in the present experiment. The residence time is the integral scale divided by the mean velocity ($\ell/\bar{U}$). Compared with jet flames, the present experiment has larger integral scales and smaller mean velocities, yielding larger residence times. Consider the case for which a vortex happens to exert a constant

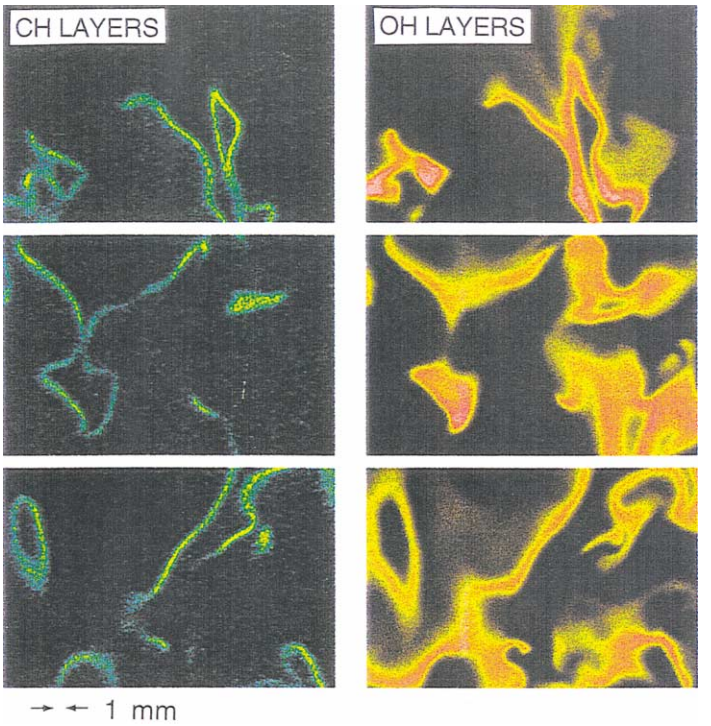

FIG. 4. Simultaneous images of the CH and the OH reaction zone layers in the IWF at three random times. Image size = 23 mm by 30 mm. Left edge of each image is the centerline; bottom edge of each image is x = 36 mm (see Fig. 1a).

flame stretch rate K during a residence time t_{res}. Using the definition of K [16],

$$K = (1/A)\, dA/dt \tag{1}$$

integration of this equation yields

$$K \cdot t_{res} = \ln(A_T/A_L) \tag{2}$$

A_T is the flame surface area after the wrinkling and A_L is the area before the wrinkling. Thus, intense wrinkling (large A_T/A_L) requires that both quantities on the left side of equation 2 be large; the stretch rates should be large, and they should be exerted for long residence times. Since stretch rates tend to scale with velocity fluctuations u' and residence time scales with $(1/\bar{U})$, the present conditions which maximize $u'/\bar{U}$ are conducive to the formation of intensely wrinkled flames.

Figure 5 is a superposition of 25 images of the CH reaction layers, which shows the structure of the turbulent flame brush. Direct observation of the flame brush might lead one to conclude that the reaction zone is thick and distributed in space; however, Fig. 5 shows that the brush is made up of many thin reaction zones. The width of the flame brush observed in Fig. 5 is approximately 22 mm wide at x = 50 mm but is only 6 mm wide near the flame base (at x = 15 mm). Properly predicting the measured flame brush thickness represents a challenge to LESs of these types of flames.

Thickness of the CH Layer and Flame Surface Density

Figure 6 quantifies the mean thickness of CH layers ($\bar{\delta}_{CH}$) in the IWF at four axial locations. In each of four regions, the normal to each CH layer was determined and the layer full width at the half-maximum intensity location was recorded. Values of $\bar{\delta}_{CH}$ vary from 0.4 mm near the flame base to 0.6 mm near the tip. These values are nearly identical to the values of $\bar{\delta}_{CH}$ that were measured in a laminar jet flame by Donbar et al. [8], in which $\bar{\delta}_{CH}$ varied from 0.4 mm near the base to 0.6 mm near the tip. Also shown in Fig. 6 are values of δ_{CH} computed for a laminar counterflow flame having nitrogen-diluted methane fuel, as in the experiment; the OPPDIF code was used with GRI-Mech 2.11 chemistry. Values of δ_{CH} for the counterflow flame decrease from 0.45 mm to 0.20 mm as strain increases from 100 s^{-1} to 1000s^{-1}. Thus the measured values of $\bar{\delta}_{CH}$ are not only similar to values measured in the laminar jet flame [8], they are similar to values computed for a counterflow flame. The values of the CH layer thicknesses $\bar{\delta}_{CH}$ in Fig. 6 are two-dimensional values and are not three-dimensional measurements. Buch and Dahm [20, Fig. 23] showed that in non-reacting flows the true three-dimensional thickness of scalar layers is typically 20% smaller than the two-dimensional measurements. Thus the true three-dimensional thickness of CH layers is ex-

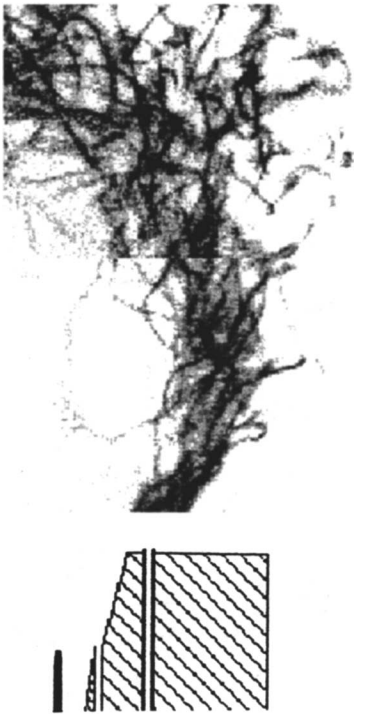

FIG. 5. Superposition of 25 images of CH layers showing the broad region in space over which the reaction layers move, due to turbulence. Imaged region is 46 mm high, 34 mm wide; left side of images is the centerline.

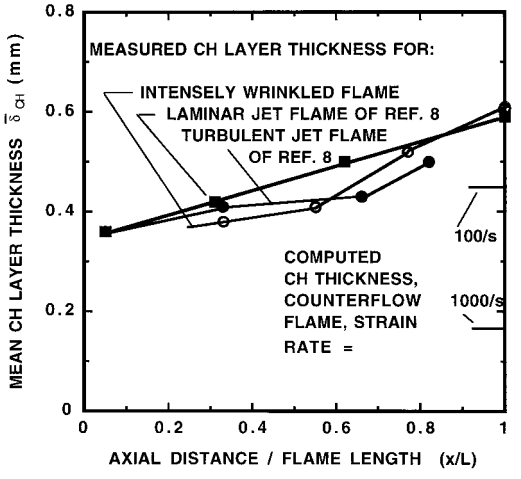

FIG. 6. Average thickness of CH layers: in the IWF, compared to values measured in a laminar jet flame and in a turbulent jet flame [8], showing that turbulence level has no effect on CH layer thickness.

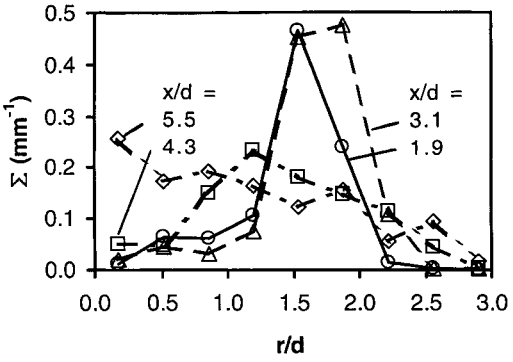

FIG. 7. Measured profiles of the flame surface density (Σ) in the IWF at various axial locations. Fuel tube diameter (d) = 10 mm.

pected to be somewhat smaller than the values in Fig. 6.

Therefore, in the present experiment, turbulence did not significantly broaden the CH reaction layers, since as the turbulence intensity ($u'/\bar{U}$) increased from zero in the laminar jet flame [8] to a large value of 3.6 in the present work, $\bar{\delta}_{CH}$ did not increase significantly. Also, an increase in the turbulence level caused the reaction layers to extinguish before they showed any signs of becoming broadened by turbulence in the present experiment. Note that the CH layer thickness is not a measure of the width of the entire fuel decomposition zone; fuel decomposition also may proceed along some chemical pathway that does not involve CH. However, CH images are useful, and the relative broadening of the zones of other fuel-decomposition reactions (involving HCO, etc.) due to turbulence should be comparable to that of CH.

The OH layers in Fig. 4 are observed to often have a thickness of approximately 1.5 to 4 mm. In the cusp regions, the OH layer abruptly thickens due to the merging of two layers. Infrequently some distributed OH reaction zones occur. It cannot be determined if broadening of the OH layers by turbulence does or does not occur. Even a laminar jet flame has a region of OH that extends several millimeters away from the flame front.

The flame surface density (Σ) is defined as $\lim(\Delta x \rightarrow 0)\ A/\Delta x^3$, where A is the average reaction zone surface area that occurs within an interrogation box of volume Δx^3. In the present work, Σ was approximated by $\lim(\Delta x \rightarrow 0)\ P/\Delta x^2$, where P is the average perimeter of the center of the CH layers that occur in an interrogation box of area Δx^2, where Δx is 2.5 mm. The surface density thus is defined herein as the surface density of the CH reaction layers; this may differ somewhat from the surface density of some other reacting species, but it does provide a useful, precisely defined number which can be com-

pared directly to values computed by LESs of the CH reaction zone surface density. Fig. 7 shows that Σ is confined to a relatively thin region (that is 5 mm thick) near the flame base, where its maximum value is 0.45 mm^{-1}. Near the flame tip, Σ is distributed over a broad zone that is approximately 20 mm thick, and it has a maximum value of 0.25 mm^{-1}.

Some computed values of Σ were reported to be in the range of 0.2 to 0.3 mm^{-1} for turbulent jet flames by Van Kalmthout et al. [16], but no computed values are yet available for IWFs. The measurements reported herein quantify the structure of the reaction layers (such as layer thickness, surface density and brush thickness) and can provide guidelines for the development of new combustion models.

Conclusions

1. Images of the CH and OH reaction zones were obtained within IWFs having turbulence intensities ($u'/\bar{U}$) of 3.6, which is 10 times the value found in turbulent jet flames. Images in the IWF regime have not been available previously. Reaction zones in the IWF regime differed from those within jet flames in that they consisted of shredded flames, which are short segments of CH and OH layers. A large number of locally extinguished regions were identified where both the CH and the OH layers abruptly disappeared. IWF reaction layers were significantly more wrinkled than layers in jet flames.
2. The CH reaction layers remained thin (0.4 to 0.6 mm) even for large values of turbulence intensity, and they had about the same thickness as CH layers in a laminar jet flame. Turbulence did not appear to either increase or decrease the thickness of the CH layers in the present experiment significantly from the laminar jet flame values.
3. Profiles of flame surface density were narrow near the flame base and had a peak value of 0.45 mm^{-1}; profiles of Σ near the flame tip were broadened over a 20 mm region and had a peak value of 0.3 mm^{-1}. Properly predicting measured value of Σ represents a challenge to new models.
4. The wrinkles in the IWF flame are comparable to the typical integral scale of 11 mm; no small-scale wrinkles less than half of the integral scale were observed.

Acknowledgments

The diagnostics facilities and support for two of the authors (JMD, CDC) was provided by the Air Force Research Labs/PRSS, Wright-Patterson Air Force Base. Fellowship support for A. Ratner was provided by the Association Francois-Xavier Bagnoud. The burner was provided by the Gas Research Institute as part of the SCALING 400 project. Data analysis support and facilities were provided by National Science Foundation Grants CTS 9123834 and CTS 9904198 administered by Dr. Farley Fisher.

REFERENCES

1. Kim, W., Menon, S., and Mongia, H. C., *Combust. Sci. Technol.* 143:25–62 (1999).
2. Menon, S., and Jou, W.-H., *Combust. Sci. Technol.* 75:53–72 (1991).
3. Dahm, W. J. A., Tryggvason, G., Frederiksen, R. D., and Stock, M. J., *Computational Fluid Dynamics in Industrial Combustion,* (C. E. Baukal, Jr., ed.) CRC Press, Boca Raton, FL, in press.
4. Tryggvason, G., and Dahm, W. J. A., *Combust. Flame* 83:207–220 (1991).
5. Bilger, R. W., *Proc. Combust. Inst.* 22:475–488 (1988).
6. Peters, N., *Proc. Combust. Inst.* 21:1231–1250 (1986).
7. Carter, C. D., Donbar, J. M., and Driscoll, J. F., *Appl. Phys. B* 66:129–132 (1998).
8. Donbar, J. M., Driscoll, J. F., and Carter, C. D., *Combust. Flame* 122:1–19 (2000).
9. Starner, S. H., Bilger, R. W., Dibble, R. W., Barlow, R. S., Fourguette, D. C., and Long, M. B., *Proc. Combust. Inst.* 24:341–349 (1992).
10. Schefer, R. W., Namazian, M., Filtopoulos, E. E. J., and Kelly, J., *Proc. Combust. Inst.* 25:1223–1231 (1994).
11. Seitzman, J. M., Ungut, A., Paul, P. H., and Hanson, R. K., *Proc. Combust. Inst.* 23:637–644 (1990).
12. Barlow, R. S., and Frank, J. H., *Proc. Combust. Inst.* 27:1087–1095 (1998).
13. Mahalingham, S., Chen, J. H., and Vervisch, L., *Combust. Flame* 102:285–297 (1995).
14. Pitsch, H., Chen, M., and Peters, N., *Proc. Combust. Inst.* 27:1057–1064 (1998).
15. Pope, S. B., and Anand, M. S., *Proc. Combust. Inst.* 20:403–410 (1984).
16. Van Kalmthout, E., Veynante, D., and Candel, S. M., *Proc. Combust. Inst.* 26:35–40 (1996).
17. Hsieh, A., Dahm, W. J. A., and Driscoll, J. F., *Combust. Flame* 114:54–80 (1998).
18. Thring, M. W., and Newby, M. P., *Proc. Combust. Inst.* 4:67–74 (1952).
19. Du, J., and Axelbaum, R. L., *Combust. Flame* 100:367–375 (1995).
20. Buch, K. A., and Dahm, W. J. A., *J. Fluid Mech.* 364:1–29 (1998).

COMMENTS

Larry Kostiuk, University of Alberta, Canada. Could you please address the concern that two-dimensional imaging techniques are unable to distinguish between fragmenting of a flame surface and out-of-imaging-plane wrinkling?

Author's Reply. The two-dimensional images can, in fact, distinguish between fragmenting and out-of-plane wrinkling. Consider a three-dimensional wrinkled flame surface that is continuous (and has no regions of extinction) which a two-dimensional light sheet intersects. The intersection of these two surfaces must form a set of closed contours, which might look like small circles or continuous lines. It is impossible for the flame contour in the two-dimensional image to abruptly end unless there is flame extinction in the three-dimensional flame surface. We believe that at the locations where we observe both the CH and OH layers to simultaneously extinguish, there must be local extinction in the three-dimensional flame surface.

•

Paul Ronney, University of Southern California, USA. You state that the CH zones are "thin." Are they thin compared to the smallest scale of turbulence, which is the usual definition of thin reaction zones in turbulent flows?

Author's Reply. When we state that the CH layers "remain thin," we mean that as the turbulence level increases the CH layers do not become any thicker than the CH layers measured in a laminar jet flame. Fig. 6 shows that the CH layers in the intensely wrinkled flame are approximately 5–10% thinner than CH layers in the laminar jet flame. No comparisons are made to the Kolmogorov scale since there is no evidence that the weak eddies that have diameters equal to the Kolmogorov scale are strong enough to affect the flame properties.